Astron. Astrophys. 360, 1148–1156 (2000)

ASTRONOMY AND ASTROPHYSICS

The effect of different ion fraction datasets on plasma diagnostics

D. Gianetti[1], **E. Landi**[2,1], **and M. Landini**[1]

[1] University of Florence, Dipartimento di Astronomia e Scienza dello Spazio, Italy
[2] Max-Planck-Institut für Aeronomie, Katlenburg-Lindau, Germany

Received 5 May 2000 / Accepted 6 July 2000

Abstract. In the present work the element abundances in an active region observed on the solar disk are studied using EUV spectral lines observed by the Coronal Diagnostic Spectrometer (CDS) on board of SOHO. Making use of the large number of lines identified in the CDS spectral range and of the instrument imaging capability, the abundances of several elements having First Ionization Potential (FIP) smaller and greater than 10eV have been determined in different parts of the observed active region. Also, the differential emission measure of the selected emitting regions have been determined.

This study has been carried out assuming ionization equilibrium in the emitting plasma, and adopting three different ion fraction datasets to interpret the observed intensities. This has permitted a detailed check of the impact of differences in the ion fraction datasets on the element abundances measurements and *DEM* determination and to assess the reliability of the use of EUV line intensities for such studies.

Our results show that the use of different ion fractions may alter significantly the measured abundances and *DEM* curves, and have large effects on quantitative FIP effect studies.

Key words: plasmas – Sun: abundances – Sun: activity – Sun: UV radiation

1. Introduction

Some of the most widely used techniques for measuring the physical parameters of optically thin plasmas involve the use of extreme ultraviolet emission line intensities. These techniques consist in comparing the observed line intensities and intensity ratios with theoretical estimates calculated as a function of the relevant physical parameter. Using these techniques, electron temperature, electron density, plasma Emission Measure and Differential Emission Measure, and element abundances have been extensively investigated in the literature. These diagnostic techniques have permitted to address some of the most important unresolved issues in the physics of the solar and stellar coronae.

However, any plasma diagnostic technique involving EUV line intensities requires the knowledge of a large amount of atomic data and transition probabilities in order to be carried out; these are necessary to calculate the theoretical line intensities for a given ion to be compared with the observations. It is also usually assumed that the plasma is in ionization equilibrium; this assumption, which can be misleading in highly dynamic plasma, allows the use of the ion fraction datasets found in the literature.

Thus, together with the atomic data and transition probabilities necessary to calculate ions' emissivity, ion fractions are a possibile source of uncertainty in plasma diagnostic studies.

The ion fractions datasets available in the literature have been calculated by a number of authors using the state-of-the-art ionization and recombination rates available at the time of publication. However, progress in the theoretical models for ionization and recombination processes have led to significant changes in ionization and recombination rates. The differences in the rates used in the calculations may cause differences in the resulting ion fractions, and therefore may have important effects on the plasma parameters determined adopting these datasets.

Electron density and temperature of optically thin plasmas are usually determined by intensity ratios between lines emitted by the same ion (Mason & Monsignori Fossi 1994), so that any effect of the ion fraction is ruled out. However, many authors have used intensity ratios from lines of different ions to determine the electron temperature in in the solar corona under different physical conditions, so that uncertainties and changes in the ion fraction need to be taken into account.

Element abundance measurements and *DEM* diagnostics are usually carried out using lines from several different ions, so that ion fractions might be an important source of uncertainty.

A few studies have been carried out in order to assess the uncertainties of ion fraction datasets and their effects on plasma diagnostics. Cheng et al.(1979a,b) compared ion abundance calculations from Jordan (1969, 1970), Summers (1974) and Jacobs et al. (1977) by means of Si VIII, Fe XI, Fe XII and Fe XXI line width studies from solar spectra. They find that observations indicate that Summers (1974) ion abundances are probably less accurate than the other two. The same conclusion has been drawn by Feldman et al.(1981) using EUV line intensities from solar flares. All these studies indicate that differences in plasma diagnostics are expected when these ion fraction datasets are used.

Send offprint requests to: E. Landi (enricol@arcetri.astro.it)

In the recent past, Masai (1997) investigated the impact of uncertainties in the ionization and recombination rates on X-ray spectral analysis, finding that differences in the rates led to significant differences in iron abundance and plasma temperature measurements. Phillips & Feldman (1997) have used *Yohkoh* flare observations to check the ion fractions of He-like ions, concluding that the observed spectra were consistent with the adopted ion fractions at the 50% level of precision, and this led to changes in plasma diagnostic results. Allen 2000 investigated the effect of different ion fraction datasets on temperature diagnostics in an isothermal, quiet solar region off the solar disc using EUV line intensities, finding that the use of different ion fractions did not alter the measured temperature values. Finally, Landi & Landini (1999) investigated the effect of different ion fractions in the calculation of radiative losses of optically thin plasmas: they found differences in the results up to 40% at coronal temperatures.

The scope of the present work is to address the problem of the effect of uncertainties in the ion fraction datasets on plasma diagnostics, in order to assess the stability of the measured plasma parameters against ion fraction uncertainties. In the present work element abundances of elements with First Ionization Potential (FIP) greater than 10 eV (high-FIP elements) and smaller than 10 eV (low-FIP elements) are measured by means of EUV spectral line diagnostics using three different ion abundance datasets. We analyze SOHO-CDS observations of an active region on the solar disk which is relatively stable in time and shows a large number of structures in the field of view. Since the three ion fraction datasets used show remarkable differences, it is expected that results will change. As the diagnostic technique used in the present work involves *DEM* analysis, the present work also allows to check the effects of different ion fractions on *DEM* diagnostics.

This check on element abundances and *DEM* diagnostics is important. In fact the *DEM* is an important physical quantity for plasma modelling of solar and stellar coronae.

Element abundances measurements are necessary to address the *FIP effect*. This effect consists in the difference between the element abundances in the solar photosphere/chromosphere and in the overlying corona, which has been observed by means of spectroscopic analysis and solar energetic particles (SEP) data. This difference seems to be related to the FIP of the elements, in the sense that the abundance of elements with FIP < 10 eV is enhanced by a factor between 3 and 4 relatively to that of elements with FIP > 10 eV. Recent reviews of this effect may be found in Feldman (1992) and Feldman & Laming (2000). Similar effects have been found in stellar spectra (Laming et al.1996; Drake et al.1997; Laming & Drake 1999).

To date, no comprehensive theory has been developed which is able to account for such a behaviour of element abundances.

The present paper is structured as follows: the basic theory of emission line intensity is outlined in Sect. 2, and a quick comparison between different ion fractions datasets of a few ions relevant to the present study is carried out in Sect. 3. The observations are described in Sect. 4; Sect. 5 reports the results, which are discussed in Sect. 6.

2. Emission line intensities

The number of photons observed in optically thin spectral line $i \rightarrow j$ is given by

$$I_{ij} = \frac{1}{4\pi}\int_h N_j\left(X^{+m}\right) A_{ji} dh \qquad ph\ cm^{-2}\ s^{-1}\ sr^{-1}. \tag{1}$$

If the *Contribution Function* $\mathrm{G}_{ij}(T, N_e)$ of the line is defined as

$$G(T, \lambda_{i,j}) = \frac{N_j(X^{+m})}{N(X^{+m})}\ \frac{N(X^{+m})}{N(X)}\ \frac{N(X)}{N(H)}\ \frac{N(H)}{N_e}\ \frac{A_{ji}}{N_e} \tag{2}$$

where

1. – $\frac{N_j\left(X^{+m}\right)}{N(X^{+m})}$ is the relative upper level population;
2. – $\frac{N\left(X^{+m}\right)}{N(X)}$ is the relative abundance of the ion X^{+m} (*ion fraction*); this quantity is taken from the literature under the assumption of ionization equilibrium;
3. – $\frac{N(X)}{N(H)}$ is the abundance of the element X relative to hydrogen;
4. – $\frac{N(H)}{N_e}$ is the hydrogen abundance relative to the electron density (≈ 0.8 for fully ionized plasmas);
5. – A_{ji} is the Einstein coefficient for spontaneous emission.

and the *Differential Emission Measure* (*DEM*) is introduced as

$$\varphi(T) = N_e^2 \frac{dh}{dT} \tag{3}$$

the number of photons emitted in a spectral line may be expressed as

$$I_{ij} = const \times \int_T G(T, \lambda_{i,j})\varphi(T) dT. \tag{4}$$

Throughout this work, use is made of the CHIANTI database (Dere et al.1997; Landi et al.1999a) and, for some ions not found in CHIANTI, of the Arcetri Spectral Code (Landi & Landini 1998a) to calculate theoretical line emissivities.

3. Ion fractions

From Eq. 2 it is possible to see that the X^{+m} ion fraction is a very important parameter for the calculation of the theoretical emitted line intensity. Ion fractions have been calculated in the literature by a number of authors, using the most accurate ionisation and recombination rates available at the time. Most of these authors have assumed that the plasma is in ionization equilibrium, and have also neglected density effects in the calculation, so that this quantity is provided as a function of electron temperature only. Improved rates have been appearing in the literature during the periods between each of the ion fraction calculations, so that the ion fractions resulting from each computation may differ significantly from the previous ones.

The ion fraction datasets which have been considered for our test are:

– Shull & Van Steenberg (1982) (hereafter SHU)

– Arnaud & Rothenflug (1985), with the more recent Fe corrections from Arnaud & Raymond (1992) (hereafter RAY)
– Mazzotta et al.(1998) (hereafter MAZ)

All these computations assume that in a low-density plasma photoabsorption and three-body recombination are negligible. Charge transfer reactions are also neglected by Shull & Van Steenberg (1992), although they can be important in low temperature plasmas. Thus, differences between RAY and MAZ are due both to improvements in the ionization and recombination data (theoretical and experimental), and in the analytical formulae used to represent the data and interpolate values for the missing ions. Shull & Van Steenberg (1982) adopt a "total" collisional ionization rate to represent both direct ionization and autoionization processes, while all the more recent works adopt two separate cross sections, leading to more accurate and physically meaningful formulae. The more recent works include a larger amount of experimental cross sections to derive their analytical formulae, so that the results should be more accurate.

3.1. Comparison of different ion fraction datasets

A quick comparison between ion fractions for several ions calculated in the SHU, RAY and MAZ dataset shows that in some cases differences are not huge, but for some ions quite dramatic changes are found between the curves provided by each of these computations. A thorough and systematic comparison of these three datasets is beyond the scope of this work; in the following only a few examples of this comparison are reported, that are relevant to the present work. These examples clearly indicate how large the differences might be in some cases, so that large effects on plasma diagnostics are expected.

Figs. 1 and 2 report the ratio between the ion fractions of Shull & Steenberg (1982) and Mazzotta et al.(1998) relative to the RAY data for a few important ions observed in the CDS spectrum. The scale in Figs. 1 and 2 is logarithmic. These figures show clearly that differences are usually of the order of 20-40% between these datasets, although for instance iron ions usually agree within 10% between Arnaud & Raymond (1992) and Mazzotta et al.(1998), in some cases differences may rise up to a factor 3-4 (Ne VII) or even to order of magnitudes (Ca X).

Given the size of the changes in the ion fraction datasets, it is to be expected that plasma diagnostics techniques based on the use of EUV emission lines will be significantly affected and will provide different results when each of these ion fraction datasets are adopted.

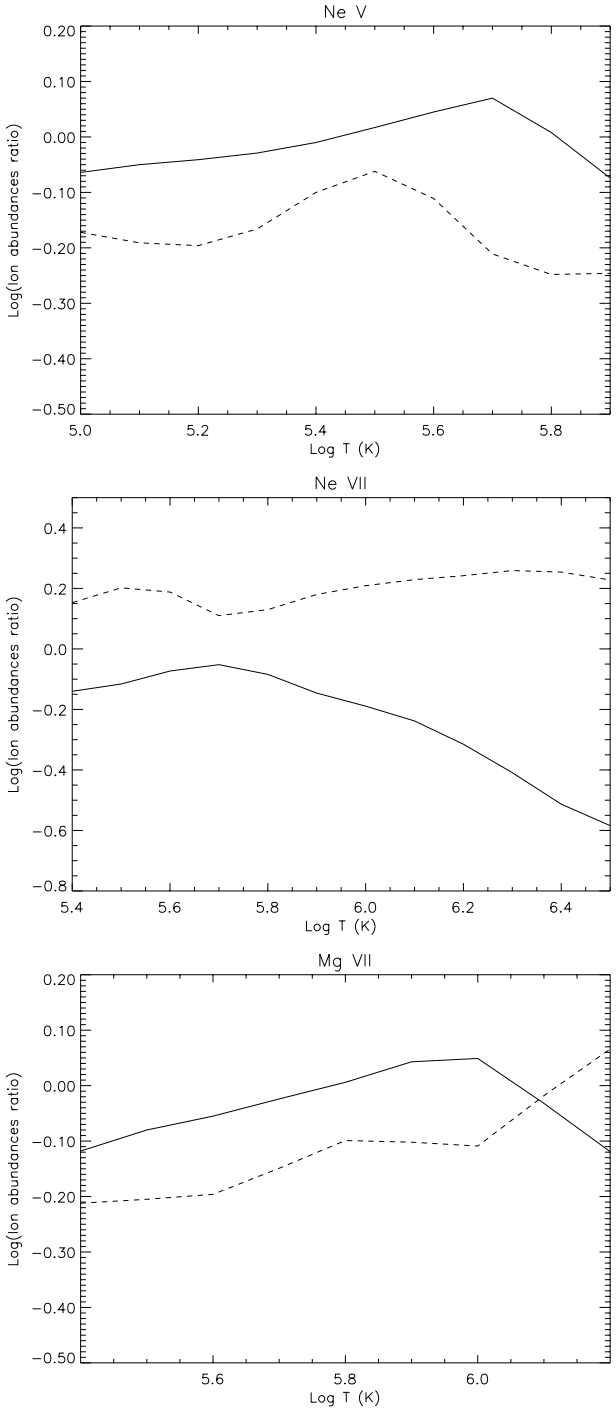

Fig. 1. Comparison for Ne V (top), Ne VII (middle) and Mg VII (bottom) ion fractions. Full line: SHU/RAY relative ion fraction; dashed line: MAZ/RAY relative ion fraction.

4. Observations

The Coronal Diagnostic Spectrometer (hereafter CDS) is an imaging spectrograph, whose primary objective is the study of the solar corona through line and continuum emission between 150 Å and 780 Å. The main achievements of CDS are therefore the large number of lines that can be observed simultaneously, the monochromatic imaging capability and the possibility of long duration studies.

CDS is composed of two distinct spectrometers sharing the same telescope: the Grazing Incidence Spectrometer (hereafter GIS) covering four spectral ranges: 151-221, 256-341, 393-492 and 659-785 Å; and the Normal Incidence Spectrometer (hereafter NIS) covering the ranges 307-379 and 513-633 Å. Full details of the CDS instrument may be found in Harrison et al. (1995). In the present work use is made both of the Normal Inci-

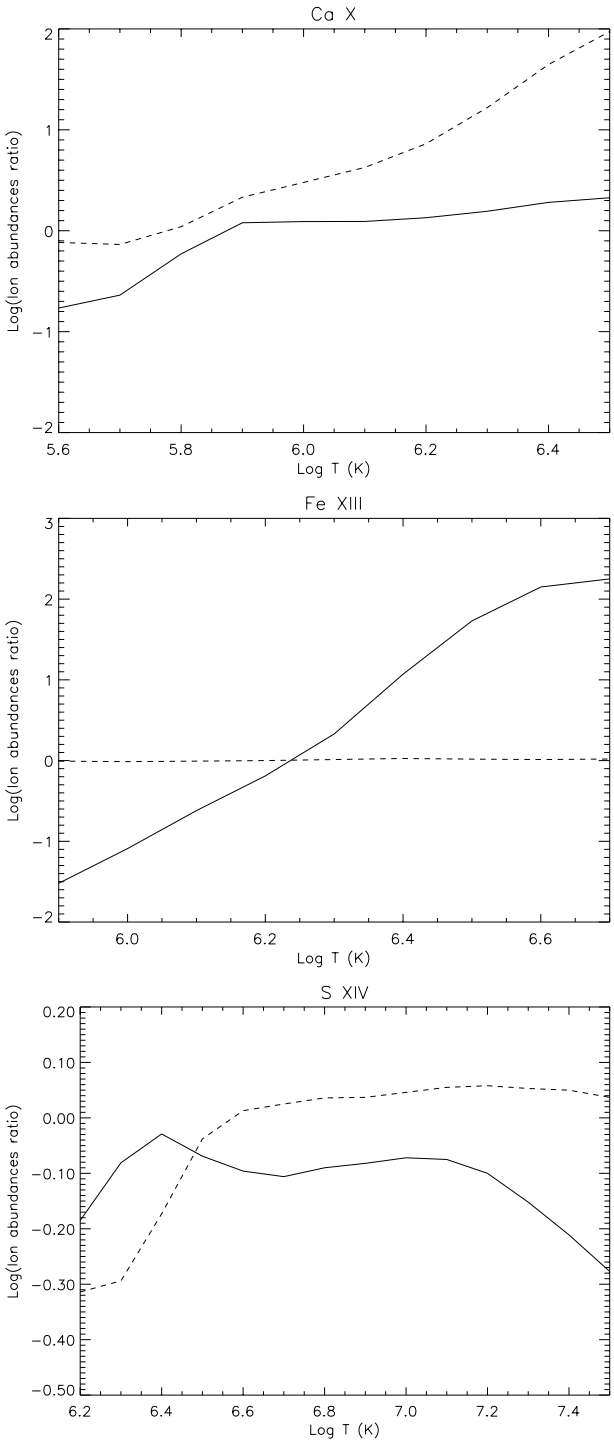

Fig. 2. Comparison for Ca X (top), Fe XIII (middle) and S XIV (bottom) ion fractions. Full line: SHU/RAY relative ion fraction; dashed line: MAZ/RAY relative ion fraction.

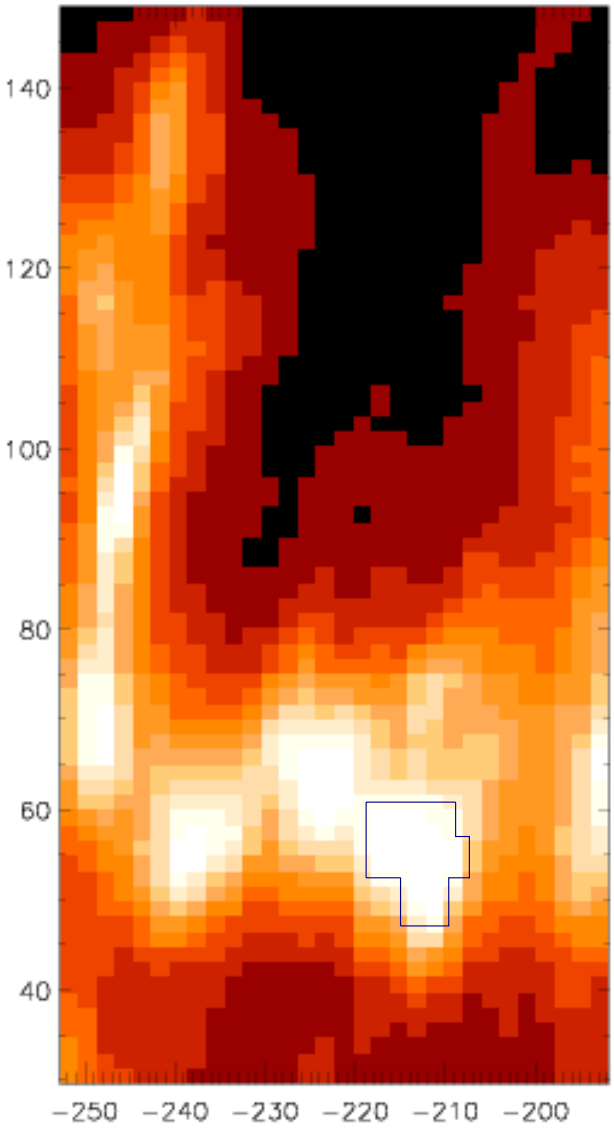

Fig. 3. CDS intensity map of the observed region observed by the He I 537 Å line. The intensity closely follows the magnetic field pattern. The contours of the portions selected for the analysis are overplotted on the map.

dence Spectrometer and of the Grazing Incidence Spectrometer in order to maximise the number of ions whose lines are observed in the spectrum.

The observations analyzed in the present work have been obtained by CDS on 19 November 1996 and consist of a full spectrum scan of NIS and a full spectrum scan of GIS. As the two instruments cannot be used simultaneously, the GIS spectrum has been observed before the NIS spectrum. The NIS field of view is 61×119 arcsec^2 and is centered at $(-222, 89)$; the GIS field of view is 61×61 arcsec^2 and is included in the NIS one.

The NIS field of view is displayed in Fig. 4 overlaid to an MDI magnetogram which shows the bipolar structure of the active region: the NIS (and GIS) field of view include only the positive polarity of the region. Figs. 3 and 5 are monochromatic images of the observed active region at He I 537 Å (around 10^4 K) and Mg X 625 Å (2.5×10^6 K).

Two smaller portions of the emitting region have been selected to be analyzed, and are overlaid in Figs. 3 and 5. They correspond to a region of enhanced magnetic field corresponding to He I enhanced emission, and to a small bright point with

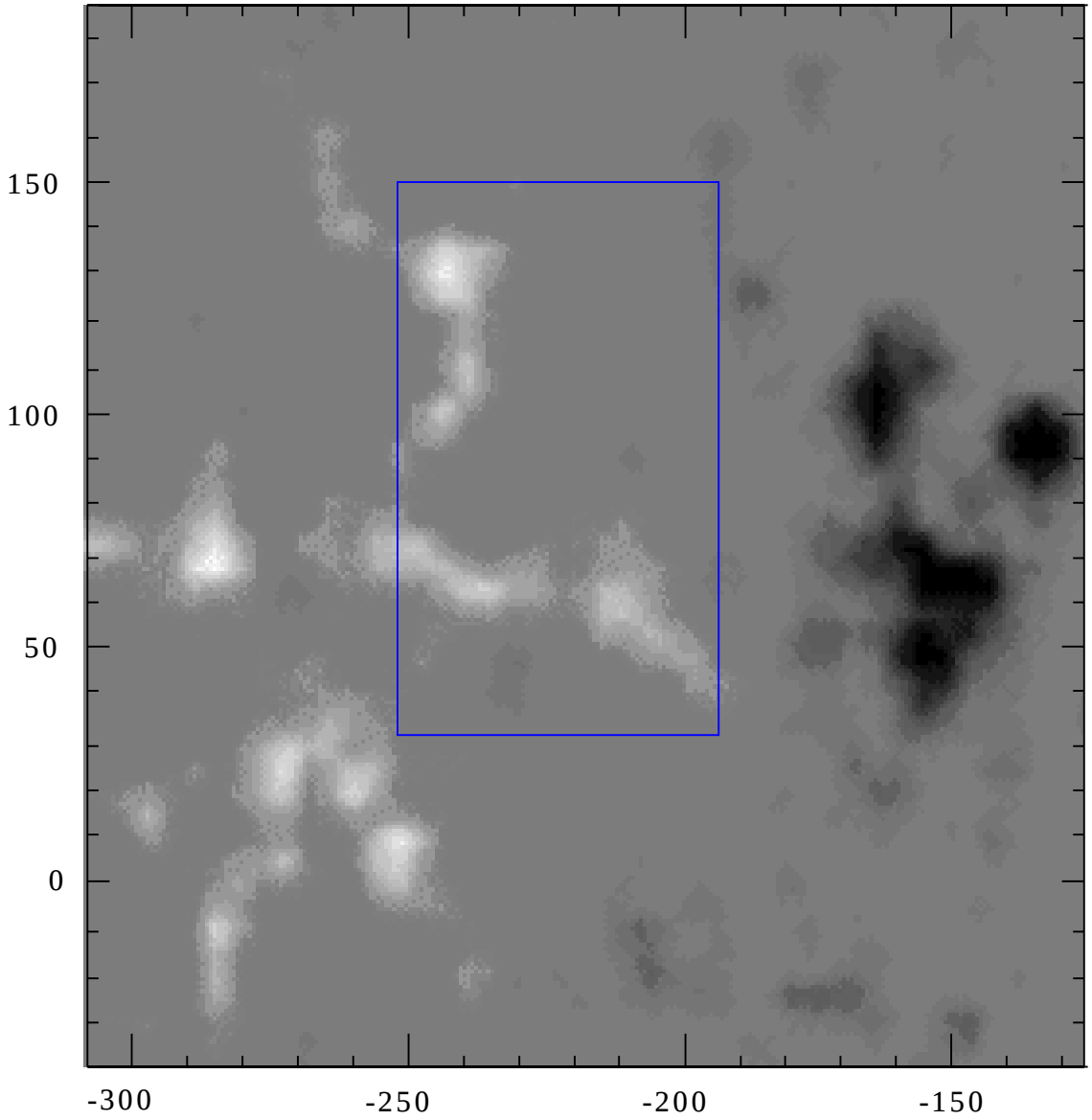

Fig. 4. MDI magnetogram of the observed active region. The CDS field of view is overlaid on the magnetogram: the CDS observation covers only the positive portion of the bipolar magnetic region.

enhanced emission in ions formed at around 8×10^5 K (visible, for example, with the Fe IX 171 Å line).

The GIS and NIS images have been coaligned using the lines between 308 and 340 Å which are observed both in the GIS 2 and NIS 1 channels. The NIS observation has been cleaned from cosmic rays and from line tilting; in the GIS observation ghosting regions have been identified and, where possible, corrected. Only GIS lines which were unambiguously identified as free of ghosts have been included in the present study. For more details on "ghosts" in the GIS spectrum, see Breeveld (1996) and Landi et al.(1999b).

Data have been calibrated according to the standard CDS calibration available in the CDS software (as of autumn 1999). A large amount of lines ($\simeq$ 70) has been used, belonging to ions sensitive to the temperature range from 10^5 K to more than 10^6 K. Table 1 lists the ions whose lines have been used in the present study. A complete list of the observed lines can be found in Landi et al.2000. Table 1 shows that lines from high-FIP (O, Ne) and low-FIP (Mg, Al, Si, Ca, Fe) elements were detected in the present dataset; S XIV is at the boundary between high and low-FIP elements, since its FIP is 10.4 eV.

5. Data analysis

There are a two main classes of diagnostic tecniques making use of EUV spectral line intensities to measure element abundances: one involving line ratios (see for example Young & Mason (1997 or Drake et al.1997), and the other involving the *DEM* of the emitting plasma (see for example Pottasch 1963; Dupree 1972; Malinovsky & Heroux 1973; Feldman 1992; Fludra & Schmeltz 1995). The latter method allows to take into

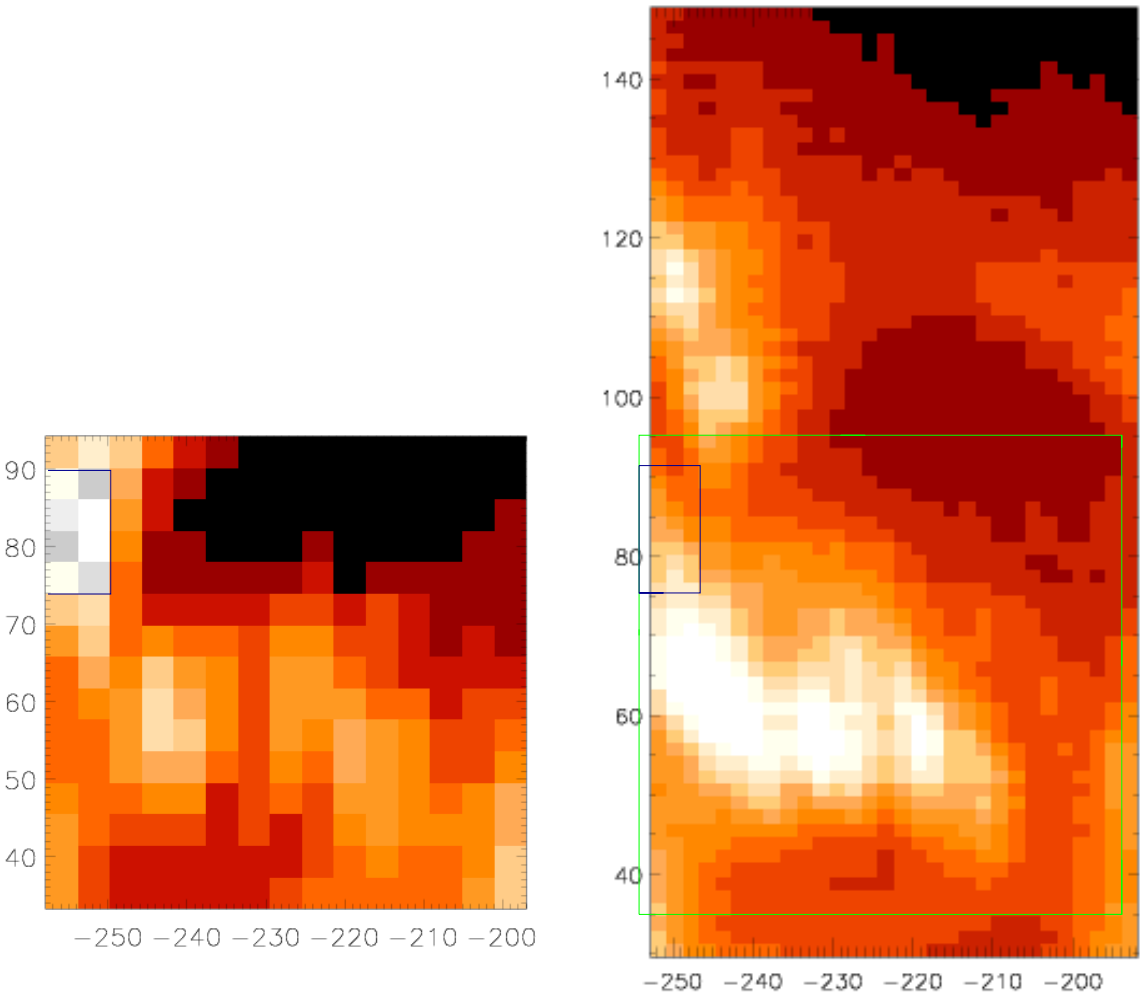

Fig. 5. CDS intensity map of the observed region observed by the Fe IX 171 Å (left) and Mg X 625 Å (right) lines. The intensity closely follows the magnetic field pattern. The contours of the portions selected for the analysis are overplotted on the map.

Table 1. Ions whose lines are used in the present analysis.

Element	FIP (eV)	Stage
O	13.6	III, IV, V
Ne	21.6	IV, V, VI, VII
Mg	7.6	V, VII, VIII, IX, X
Al	6.0	XI
Si	8.2	IX, X, XII
S	10.4	XIV
Ca	6.1	X
Fe	7.9	X, XI, XV, XVI

proper account the temperature dependence of the *Contribution Function* of the emitting ions. Since we are studying lines emitted by ions formed at different temperatures, the latter method is more appropriate for our purposes.

The *DEM* diagnostic technique we adopt is described in full detail by Landi & Landini (1997). This diagnostic technique relies on an iterative procedure which calculates a temperature-dependent correction to an initial arbitrary *DEM* , until theoretical line intensities predicted through the resulting *DEM* agree with their observed values within the experimental uncertainties. The element abundance diagnostic technique adopted in the present work requires as input an adopted abundance dataset, and enables the determination of correction factors (a simple multiplicative constant) to single element abundances relative to an element, that is taken as reference.

We have used as starting values the coronal abundances of Feldman (1992). This dataset presents low-FIP element abundances enhanced by nearly a factor 4 relatively to photospheric values. During the present study the abundances of Fe has been taken as reference (correction equal to unity) and those of the other elements have been multiplied by the correction factor that gives the best fit.

5.1. DEM diagnostics

Figs. 6 and 7 display the resulting *DEM* curves for each of the two selected regions. The two regions present *DEM* curves showing qualitatively the same behaviour, with a large peak at around 1.8×10^6 K, and a high-temperature tail which rapidly decreases as temperature exceeds 3×10^6 K. Similar *DEM*

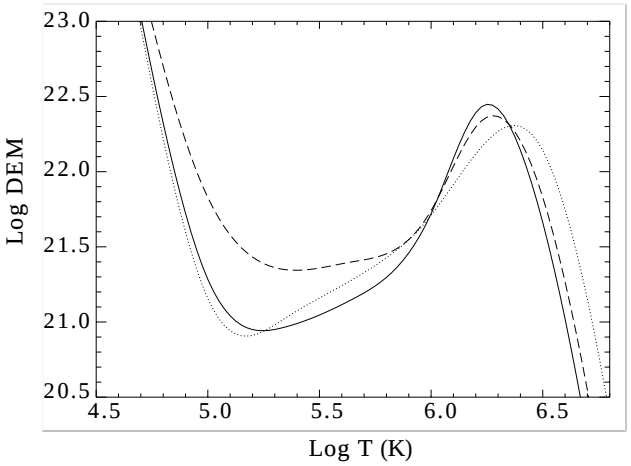

Fig. 6. *DEM* for the He I selected region, as determined using three different ion fractions datasets as described in the text: RAY (full line), SHU (dotted line) and MAZ (dashed line).

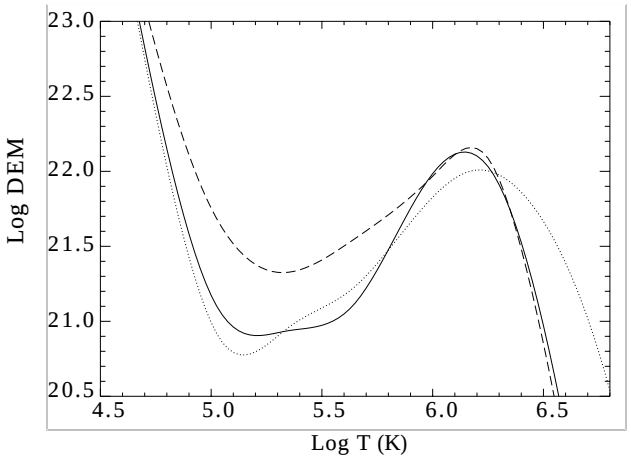

Fig. 7. *DEM* for the Fe IX selected region, as determined using three different ion fractions datasets as described in the text: RAY (full line), SHU (dotted line) and MAZ (dashed line).

curves have been found by a number of authors in the literature.

From Figs. 6 and 7 it is evident that the use of different ion fraction datasets hugely affects the shape of the *DEM* curves at all temperatures. For example, in both the emitting regions the RAY and MAZ datasets provide similar curves at temperatures around 1-1.5$\times 10^6$ K, but large differences are found at transition region and chromospheric temperatures. On the contrary, SHU and RAY curves provide a reasonable good agreement at low temperatures, but heavily disagree at coronal temperatures, where the peak found in the SHU *DEM* curve is broader, lower and slightly hotter than the one found in the RAY results. No agreement at all is found between the SHU and MAZ results. Differences rise up to a factor 4.

These differences are directly related to the differences in the ion fractions. For instance, the *DEM* curve at coronal temperature is mainly dominated by the Fe lines and a few other hot ions, for which Mazzotta et al.(1998) and Arnaud & Raymond (1992) provide very similar ion fractions (see for example Fig. 2): this explains the agreement found between MAZ and RAY curves at coronal temperature. Shull & Steenberg (1982) ion fractions for coronal ions, based on less accurate ionization and recombination rates, are sometimes very different from the other two datasets, so that huge differences in the *DEM* are found.

Similarly, differences found between RAY and MAZ *DEM* curves at transition region temperatures may be explained by differences in the ion fractions for the neon and magnesium ions which determine the *DEM* at those temperatures (see for example Fig. 1).

It is therefore clear that ion fraction datasets are a critical parameter in the determination of *DEM* curves from EUV emission lines, and the choice of the adopted dataset can be the dominant source for uncertainties in the results. Given the considerable size of the differences, this is particularly important for theoretical models involving the *DEM* of the emitting plasma.

Table 2. Correction factors to the Feldman (1992) element abundances for the He I (left) and Fe IX (right) emitting regions obtained using the three different ion fraction datasets RAY, SHU and MAZ. Fe abundance has been takes as reference. The FIP is in eV. The correction factors are multiplicative contants.

Ion	FIP	**RAY**	**SHU**	**MAZ**	**RAY**	**SHU**	**MAZ**
O	13.6	2.0	2.0	0.7	1.8	2.0	0.6
Ne	21.6	2.2	2.0	1.1	2.4	2.1	1.1
Mg	7.6	1.0	1.0	0.9	0.6	0.9	0.5
Al	6.0	1.0	1.2	1.0	1.0	1.2	1.1
Si	8.2	0.65	0.8	0.7	0.8	0.8	0.8
S	10.4	0.8	0.5	0.9	1.2	0.7	1.1
Ca	6.1	5.4	4.8	1.5	4.4	4.4	1.2
Fe	7.9	1.0	1.0	1.0	1.0	1.0	1.0

Unfortunately, the lack of an independent measurement of the *DEM* does not allow us to determine which of the adopted ion fraction datasets is more accurate and therefore recommendable for further *DEM* studies, or to point out ions for which new and improved calculations of ionization and recombination rates are required.

5.2. Abundance measurements

In order to determine the *DEM* curves displayed in Figs. 6 and 7 it has been necessary to correct the abundances of nearly all the elements in the dataset. Table 2 reports the correction factors to the Feldman (1992) abundances for each of the selected regions. The uncertainties of these factors are of the order of or smaller than 25%, and are given both by the uncertainties on the measured line fluxes and in the atomic data and transition probabilities used to calculate level populations (Eq. 2).

Table 2 shows that for each given ion fraction dataset, the two different regions show very similar correction factors, indicating that their element abundances are about the same despite their different position in the active region.

From Table 2 it is possible to see that the use of different ion fraction datasets may cause large differences in the abundance correction factors found in each of the two emitting regions.

The largest differences are reported for the two high-FIP elements oxygen and neon: while correction factors obtained from RAY and SHU are similar, differences of more than a factor 2 are found when they are compared to MAZ's values. It is important to note that the correction factors obtained from the MAZ ion fractions indicate also that a large correction in the relative O/Ne abundance is required, which is much greater than the value reported by Landi & Landini (1998b).

Sulphur (whose FIP is at the boundary between the high- and low-FIP classes) also shows that SHU ion fractions cause large differences in the abundance correction factors from MAZ and RAY results.

More limited differences are found for the low-FIP elements. The only exception to this is calcium, since its correction factor changes by a factor larger than 3 if MAZ ion fractions are used. It is possible to see that the use of MAZ data leads to a correction factor for calcium abundance similar to those of the other low-FIP elements, while the other two ion fraction datasets caused its value to be very large. The only calcium lines available in the CDS-NIS spectral range are due to Ca X. Anomalies in the behaviour of the Ca X lines have already been noted in previous studies (Landi & Landini 1998b and Del Zanna & Bromage 1999) and they were ascribed mostly to element abundance. These results show that ion fractions could be responsible for most of the calcium anomalies. The comparison with the behaviour of the other low-FIP elements seems to suggest that MAZ ion fractions for Ca X should be more reliable than the other two datasets, as abundances of elements belonging to the same FIP class are expected to to have qualitatively the same behaviour. This is consistent with the results of Smith et al.(1985), who pointed out that the dielectronic recombination rates used in the SHU and RAY are incorrect for the Ne-like ions, and that this altered the corresponding Na-like ion abundances. This might explain why results obtained with the MAZ dataset, who adopt different rates for Ne-like dielectronic recombination, show that Ca X is in better agreement with observations.

As in the *DEM* studies, these differences may be explained by comparisons between the ion fractions of the ions involved in the abundance measurements. Figs. 1 and 2 clearly show that huge changes are found for Ca X ion fraction between Mazzotta et al.(1998) data and those from Arnaud & Rothenflug (1985) and Shull & Steenberg (1982), which are similar; such discrepancies are found (although smaller in size) for several magnesium and neon ions.

The most important result shown in Table 2 is that the relative low-to-high FIP element abundance is heavily affected by changes in the ion fraction dataset. In particular, the use of RAY and SHU datasets show that the abundance for the high-FIP elements must be increased relative to the low-FIP elements' value, thus implying that the FIP effect is less effective than assumed by adopting the Feldman (1992) element abundances. On the contrary, results obtained using MAZ data show that the FIP effect is as strong as reported by Feldman (1992).

It is therefore clear that the ion fraction datasets are a very important source for uncertainty in quantitative FIP effect studies when EUV line intensities are used.

Unfortunately, it is not possible to carry out an independent check of the element abundances in the emitting plasma with the present data, so that it is not possible both to determine which of the ion fraction datasets is to be recommended for further studies, and to draw any quantitative conclusion on the element abundances and the FIP effect of the emitting regions.

6. Conclusions

In the present work, a SOHO-CDS observation of an active region has been used to determine the element abundances and the *DEM* of the emitting plasma by means of EUV line intensities. During the study, three different datasets for the ion fractions have been adopted in turn, under the assumption of ionization equilibrium. Since these ion fraction datasets (Shull & Van Steenberg 1982; Arnaud & Rothenflug 1985 with the latest revisions for iron from Arnaud & Raymond 1992; and Mazzotta et al.1998) show significant differences for several ions relevant to the present analysis, the present work allows us to check the effects of uncertainties in the ionization and recombination rates on plasma diagnostics.

The present work shows that the differences found in the ion fraction datasets adopted in the analysis cause large effects in the measurements of plasma physical quantities when diagnostic techniques involving EUV line intensities are used. Both the *DEM* curves and the element abundances determined in the present analysis show significant variations according to the different ion fraction dataset adopted in the analysis.

From these results, two main points can be stressed.

The first point concerns differences in the *DEM* curves. These can be significant, and can be found for any value of the electron temperature, according to the ion fraction dataset used. This may have great effects on theoretical models in the case the *DEM* curves are used for plasma modeling. This is expecially true at transition region temperatures, where the differences in the curves are largest.

The second point concerns the large differences found in the relative low-FIP/high-FIP abundance corrections. These can significantly alter any quantitative conclusion drawn on the FIP effect, as the factor around two between the results found adopting in turn each ion fraction dataset is comparable in size to the factor between 3 and 4 difference between solar photospheric and coronal low-FIP/high-FIP relative abundance.

These results show that the choice of ion fractions for plasma diagnostics is an important source of uncertainties for plasma diagnostics.

Allen et al.2000 report that using the same three ion fraction datasets considered in the present work no difference was found in electron temperature diagnostics at the solar limb. Allen et al.2000 measured the electron temperature by means of three different plasma diagnostic techniques: line intensity ratios, *DEM* analysis and a variant Emission Measure analysis. The agreement they find in temperature values when ion frac-

tions are changed is probably due to the fact that the plasma analyzed by Allen et al.2000 is isothermal, while the disk spectrum analyzed in the present study is formed by plasma whose temperature ranges from chromospheric to coronal values, so that the temperature dependence of ion fractions must be fully taken into account.

As a consequence of this work, we stress the need of new and accurate ionization and recombination rates in order to obtain more reliable calculations of ion fraction datasets, so that the uncertainty that this fundamental parameter provides to the diagnostics results can be minimized.

Acknowledgements. SOHO is a mission of international cooperation between ESA and NASA. One of the authors (EL) acknowledges support from the Italian Space Agency (ASI).

References

Allen R., Landi E., Landini M., Bromage G.E., 2000, A&A 358, 332
Arnaud M., Rothenflug R., 1985, A&AS 60, 425
Arnaud M., Raymond J., 1992, ApJ 398, 394
Breeveld A.A., 1996, Ph.D. Thesis, University of London
Cheng C.-C., Doschek G.A., Feldman U., 1979a, ApJ 227, 1037
Cheng C.-C., Feldman U., Doschek G.A., 1979b, ApJ 233, 736
Del Zanna G., Bromage B.J.I., 1999, J. Geoph. Res. 104, 9753
Dere K.P., Landi E., Mason H.E., et al., 1997, A&AS 125, 149
Drake J.J., Laming J.M., Widing K.G, 1997, ApJ 478, 403
Dupree A.K., 1972, 178, 527
Feldman U., Doschek G.A., Cowan R.D., 1981, MNRAS 196, 517
Feldman U., 1992, Phys. Scr. 46, 202
Feldman U., Laming J.M., 2000, Phys. Scr. 61, 222
Fludra A., Schmeltz J.T., 1995, ApJ 447, 936
Harrison R.A., Sawyer E.C., Carter M.K., et al., 1995, Solar Physics 162, 233
Jacobs V.L., Davis J., Kepple P.C., Blaha M., 1977, ApJ 211, 605
Jordan C., 1969, MNRAS 142, 501
Jordan C., 1970, MNRAS 148, 17
Laming J.M., Drake J.J., Widing K.G., 1996, ApJ 462, 948
Laming J.M., Drake J.J., 1999, ApJ 516, 324
Landi E., Landini M., 1997, A&A 327, 1230
Landi E., Landini M., 1998a, A&AS 133, 411
Landi E., Landini M., 1998b, A&A 340, 265
Landi E., Landini M., 1999, A&A 347, 401
Landi E., Landini M., Dere K.P., Young P.R., Mason H.E., 1999a, A&AS 135, 339
Landi E., Del Zanna G., Landini M., et al., 1999b, A&A 135, 171
Landi E., Gianetti D., Landini M., 2000, A&A in preparation
Malinovsky L., Heroux M., 1973, ApJ 181, 1009
Masai K., 1997, A&A 324, 410
Mason H.E., Monsignori Fossi B.C., 1994, Astr. Astroph. Rev. 6, 123
Mazzotta P., Mazzitelli G., Colafrancesco S., Vittorio N., 1998, A&AS 133, 403
Phillips K.J.H., Feldman U., 1997, ApJ 477, 502
Pottasch S.R., 1963, ApJ 137, 945
Shull J.M., Van Steenberg M., 1982, ApJS 48, 95 and ApJS 49, 351
Smith B.W., Raymond J.C., Mann J.B., Cowan R.D., 1985, ApJ 298, 898
Summers H.P., 1974, MNRAS 169, 663
Young P.R., Mason H.E., 1997, Solar Physics 175, 523